Fabrication of Ag Nanoparticle–Encapsulating Multilayer Films Based on PAMAM Dendrimers with Covalent Interlayer Linkages

Yufei Luo,[1] Yuan Li,[1] Xinru Jia,[1] Huaquan Yang,[1] Ling Yang,[1] Qifeng Zhou,[1] Yen Wei[2]

[1]*College of Chemistry and Molecular Engineering, Peking University, Beijing 100871, China*
[2]*Department of Chemistry, Drexel University, Philadelphia, Pennsylvania 19104*

Received 27 December 2001; revised 15 July 2002; accepted 22 October 2002

ABSTRACT: Ag-dendrimer nanoclusters were prepared with Ag^+ and carboxyl shell (G4.5) poly(amino amine) dendrimers. Self-assembly photosensitive ultrathin films were then fabricated with these Ag-dendrimer nanoclusters as polyanions and diazoresin (DR) as polycation. With UV irradiating the films became stable because of the formation of covalent linkages between the layers. Compared to similar films containing no Ag nanoclusters, the obtained films showed greatly enhanced electric conductivity. © 2003 Wiley Periodicals, Inc. J Appl Polym Sci 89: 1515–1519, 2003

Key words: conducting polymers; nanocomposites; self-assembly

INTRODUCTION

With the development of dendrimer science, chemists have taken full advantage of the unique structure and chemical properties of dendrimers to extend their theoretical and practical applications in various fields.[1,2] The preparation of a range of metallic nanoparticles with dendrimers as templates has been reported. For example, Crooks and coworkers[3] reported the formation of a regime of Au colloids 2-3 nm in size in the presence of poly(amino amine) (PAMAM) dendrimers. Tomalia et al.[4] demonstrated the preparation of a stable dendrimer/metallic copper nanocomposite with unprecedented stability in both water and methanol. Esumi and colleagues[5] generated various PAMAM dendrimers with surface amino groups as well as carboxyl groups in order to prepare Au, Pt, and Ag nanoparticles in aqueous solution. Tripathy et al.[6] reported the deposition of a multilayer thin film composed of gold–dendrimer nanoclusters and PSS and the characterization of its highly uniformed nanoscale array. However, searching for new technology to endow the films with both special function and stability remains intriguing because of the potential practical use of dendrimers. In a previous work[7] we studied covalently stabilized self-assembly films consisting of PAMAM dendrimers and diazoresin. As an extension of this research, in the current study our purpose was to assemble stable ultrathin films with metal–dendrimer composites and to explore the properties of the obtained films.

Here we report for the first time on the fabrication of self-assembly ultrathin films using Ag–PAMAM dendrimer nanocomposites as polyanions and diazoresin (DR) as polycation. The conversion of the nature of the linkage between layers from electrostatic to covalent and the stability of the films toward polar solvents were studied and are expounded here in detail. Also, the electric conductivity of the obtained ultrathin films was measured, and the results showed a potential application for these films in nanoelectronic devices.

EXPERIMENTAL

G4.5 PAMAM dendrimers were synthesized according to the literature procedures.[8]

G4.5 PAMAM ^{1}H-NMR (D_2O): Δ = 3.617 (—COOC**H**$_3$), 3.22–3.33 (—CONC**H**$_2$), 2.57–2.91 (—NC**H**$_2$), 2.37(—C**H**$_2$CO)].

After being hydrolyzed with NaOH, the methylester groups of G4.5 PAMAM dendrimers were converted to carboxylate groups (PAMAMC). The disappearance of the signal at 3.617 ppm showed there was a change in the nature of the external groups from ester to carboxylate.

Ag dendrimer nanoparticles were prepared according to the methods described in the literature.[6] The formation of Ag dendrimer nanoparticles was supported by the peak that appeared at 415 nm in the UV–vis spectrum and by transmission electron microscopy (TEM; Fig. 1). DR was prepared according to

Correspondence to: X. Jia (xrjia@chem.pku.edu.cn).
Contract grant sponsor: NSFC; contract grant numbers: 59973001, 29992590.

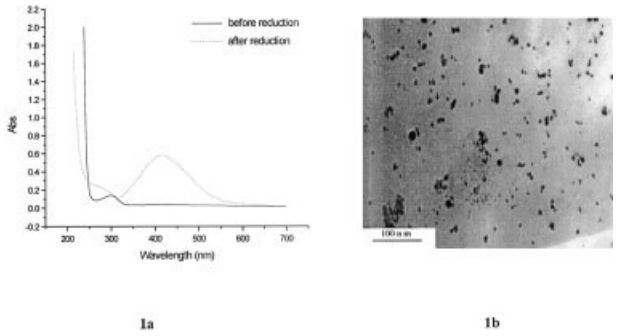

Figure 1 (a) UV–vis absorption spectrum of Ag–PAMAM (G4.5) nanocomposites in an aqueous solution; (b) TEM image of Ag–PAMAM nanocomposites.

the method described elsewhere.[9] A fresh quartz wafer was used as the substrate. After treatment with H_2SO_4 and H_2O_2 (3:1) to remove impurities on the surface, the wafer was immersed in a deionized aqueous solution of DR (2 mg/mL) for 5 min and then rinsed with deionized water and dried. Subsequently, it was dipped into the deionized aqueous solution of Ag–PAMAMC (G4.5) nanocomposites (0.5 mg/mL) for 15 min, then rinsed and dried again. Repetition of this cycle six or seven times resulted in the formation of a 12- or 14-bilayer films on both sides of the substrate. All the experiments were carried out at a constant temperature of 20°C in the dark.

To monitor the self-assembly process and the stability of the films against etching, the UV absorbance of the films on the quartz wafer after each cyclic deposition or after etching was recorded on a UV–vis scanning spectrophotometer (Shimadazu UV–2101 PC) with a selected scan range (200–500 nm). Each sample was measured 2–3 times to ensure the reliability of the results.

The surface morphology of the films was visualized by atomic force microscopy (AFM). The sample for AFM measurement was a six-bilayer film fabricated on quartz wafer, which was glued to a glass slide. The measurements were carried out in air at ambient temperature on a Nanoscopy IIIA AFM (Digital Instruments, Inc.) in the tapping mode. Commercial silicon probes (model TESP-100) were used to obtain the image, with a typical resonant frequency of around 300 kHz. All the results were calculated from a randomly selected 1 μm^2 (1 $\mu m \times 1$ μm) area on the samples.

X-ray photoelectron spectroscopy (Vgescalab 5 multitechnique electron spectrometer) was used to analyze the surface element composition of the 10- and 11-layer films fabricated from Ag–PAMAMC (G4.5) and DR.

The solvent etching experiments were performed following the literature procedure.[10–13] The 6-bilayer films were immersed in an NaCl (1*M*) aqueous solution for different times. To observe their stability toward etching, the resulting films were examined for

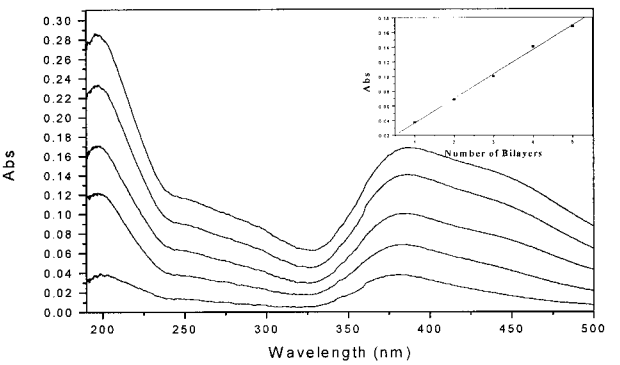

Figure 2 UV–vis absorption spectra of Ag–PAMAM/DR nanocomposite multilayers on a quartz slide. Curves correspond to absorbance of bilayers [bilayer number (bottom to top): 1, 2, 3, 4, 5]. Inset: increase in absorbance at 385 nm with number of bilayers.

UV–vis absorbance. To confirm formation of interlayer covalent bonding, the spectra of unirradiated and irradiated films fabricated on CaF_2 were recorded on a Nicolet Magna IR-750 spectrophotometer.

RESULTS AND DISCUSSION

Each cyclic deposition of the film growth was tracked with a Shimadazu UV2101 PC UV–vis scanning spectrophotometer. Figure 2 shows the UV–vis curves of the fabricated films with various bilayer numbers. As shown in the inset of Figure 2, the absorption of diazonium groups of DR at 383 nm increased linearly with an increase in the number of bilayers. This indicates that the growth of the film was smooth and uniform.

Subsequently, the film was treated with UV irradiation (360 nm), 230 $\mu W/cm^2$, so as to immobilize the Ag particles on the film. This process was also monitored with a UV–vis spectrometer. As shown in Figure 3, it is clear that the peak of the diazonium groups at

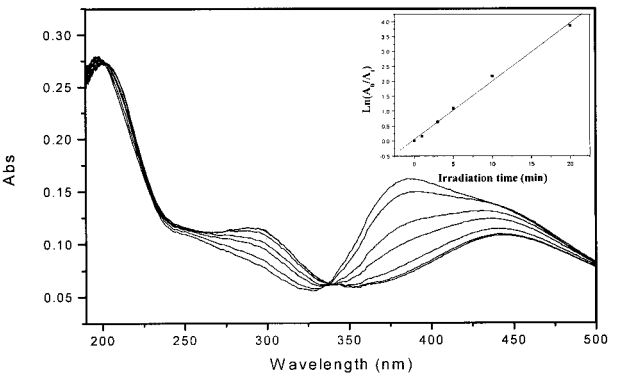

Figure 3 Relationship between UV–vis spectra of 10-layer film and UV irradiation time [Irradiation time (top to bottom): 0, 1, 3, 5, 10, 20, and 30 min]. Inset: attenuation of multilayers' absorption in 385 nm with time corresponding to first-order kinetic equation.

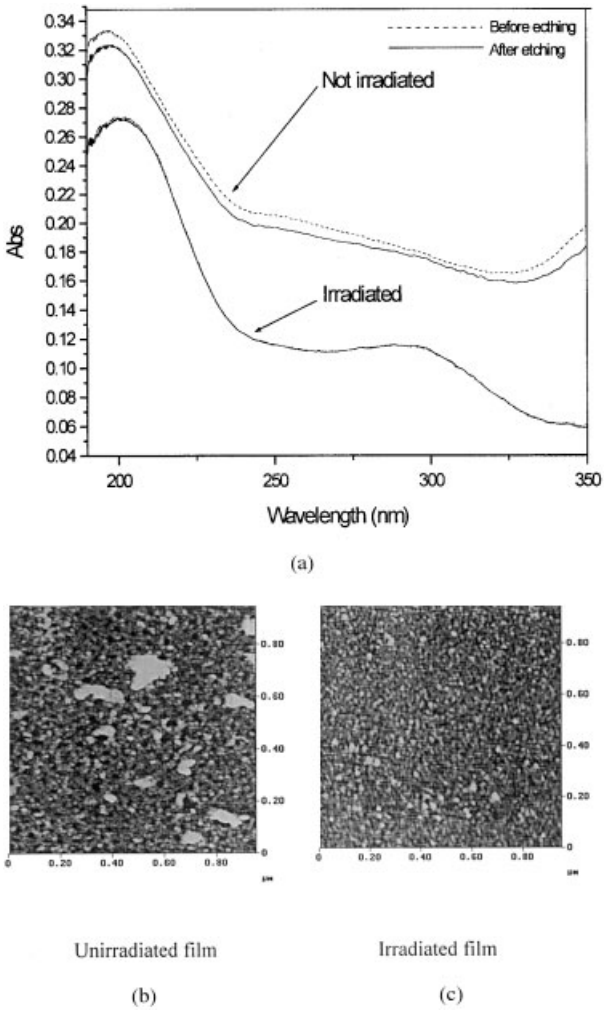

Figure 4 Etching of irradiated and unirradiated multilayer film in saturated NaCl solution (1 h): (a) UV–vis spectrum; (b) AFM image of film before irradiation, and (c) AFM image of film after irradiation.

384 nm decreased rapidly with irradiating time. The linear relationship between $\ln[(A_0 - A)/(A_t - A)]$ and time, shown in the inset of Figure 3, was verification that the decomposition reaction followed first-order reaction kinetics (A is the absorbance of the film at 384 nm).

The decomposition of the diazonium groups accompanied the change in the nature of the linkage between layers (Scheme 1{SCHEME 1}). Two facts provide support for this assumption: (1) in the IR spectrum the

TABLE I
Relative Content of Carbon, Nitrogen, and Silver in Ag–PAMAM/DR Multilayers Detected by XPS (Scan Angle 60°, Scan Depth 5μÅ)

	C	N	Ag
10-layer film (Ag–PAMAM surfaced)	1000	67.7	16.9
11-layer film (DR surfaced)	1000	96.3	—

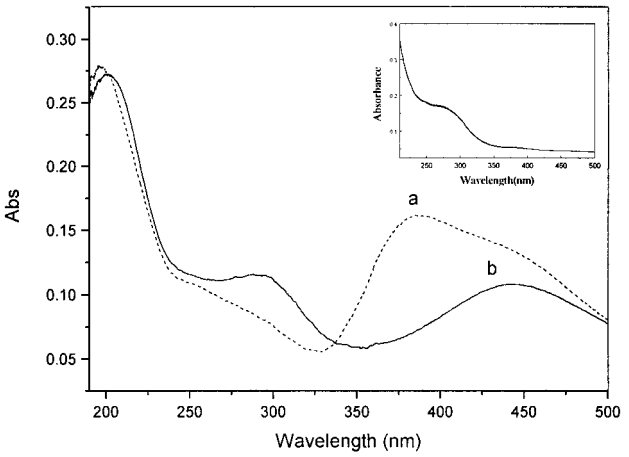

Figure 5 UV–vis spectra of a 10-layer film (a) before and (b) after irradiation. Inset: UV–vis spectra of same-type film that does not contain Ag.

stretching vibrations of the diazonium groups at 2162 cm^{-1} and the carboxyl groups at 1580 cm^{-1} disappeared after irradiating. A weak and broad peak ranging from 1640 to 1720 cm^{-1} was observed, which was assigned mainly to the carboxyl group of the ester bond; (2) it is well known that films assembled via electrostatic interaction are unstable in strong electrolyte aqueous solutions. In our experiment both films, those before and after UV irradiation, were soaked in the saturated NaCl solution for 1 h and then observed with UV–vis spectroscopy and AFM. As shown by the results displayed in Figure 4(a–c), the film before irradiation obviously was destroyed [Fig. 4(b)] after 1 h of etching. In sharp contrast, the irradiated film showed excellent resistance to the same process. The surface of the film was still smooth after etching [Fig. 4(c)], and mean roughness was around 0.4–0.9 nm according to AFM measurements.

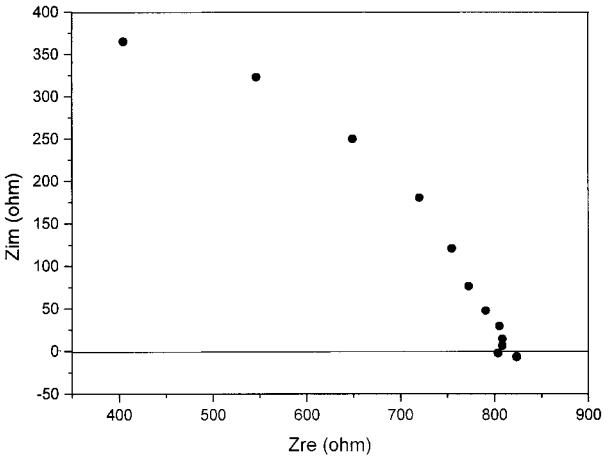

Figure 6 Impedance spectra of 50-bilayer film of Ag–PAMAM/DR.

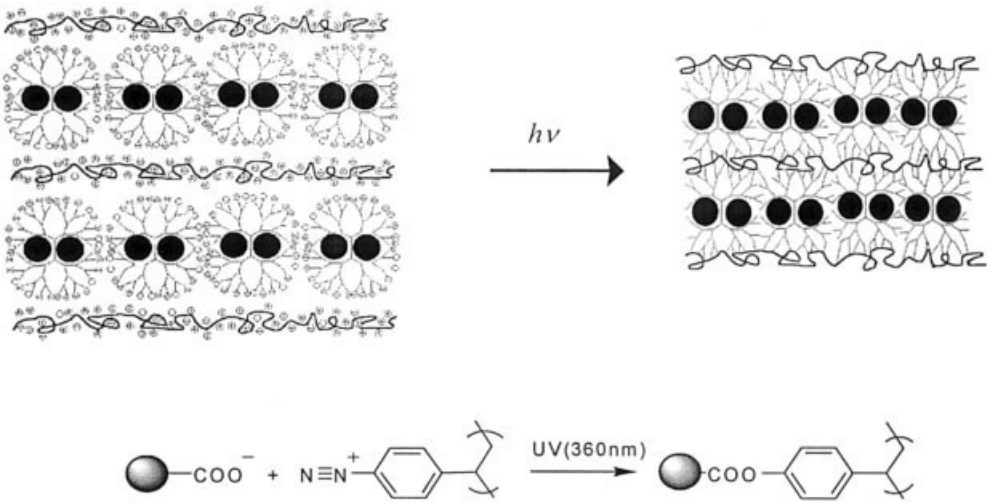

Scheme 1

To answer the question of whether the Ag nanoparticles were still encapsulated in PAMAM dendrimers and attached on the film after these procedures, elemental composition of the films on different surfaces was determined via X-ray photoelectron spectroscopy. As shown in Table I, carbon, nitrogen, oxygen, and silver were found on the 10-layer film's surface (dendrimer layer), but on the surface of the 11-layer film (DR layer), silver could not be observed. This indicates that the Ag nanoparticles were contained in the films, mainly encapsulated in the dendrimer layers.

Additional support for Ag being encapsulated in the film was what the UV–vis spectrum showed after the film underwent UV irradiating: the emergence of a peak at 415 nm (Fig. 5). This peak did not appear in the UV–vis spectrum of identical-type PAMAM–DR films. Therefore, it must have originated from the existence of the Ag nanoparticles. Interestingly, the peak had a 30-nm red shift compared with the corresponding one of the Ag–PAMAM solution. A very similar phenomenon also was found by Tripathy et al. in their experiment.[6] When they constructed Au–PAMAM composite films, a 20-nm red shift was observed and attributed to the change in the dielectric environment of gold particles in the films. In our case the red shift derived from at least two main factors. In addition to the one Tripathy demonstrated, the other factor may lie in the size effect. Crooks et al.[13] found that in the Cu–PAMAM nanocomposite solution, the plasma band was red-shifted, most likely because of the larger size of the colloids prepared with lower-generation PAMAM dendrimers. During fabrication of the films, Ag nanoparticles may be incarcerated within the dendrimers or close to the dendrimer surface because Ag^+ ions could be strongly adsorbed on the carboxyl-terminated dendrimers via electrostatic attractive force. The Ag nanoparticles near the surface can then be embedded via electrostatic force in "cages" formed between the negatively charged carboxylate groups of PAMAMC and the positively charged diazoresin groups of DR (Scheme 1). The TEM image (Fig. 1) shows that the diameter of the Ag nanoparticles ranged from 4 to 10 nm. It is possible that particles smaller than the holes of the cages would be washed out more easily in every rinse procedure. Therefore, the average size of the particles encapsulated in the film would be larger than that of the particles in solution, causing plasma band shifts to longer wavelengths.[14,15]

Electric conductivity of the films was measured in parallel-connection measurement mode using a Potentiostat/Galvanostat Model 283 tester over a frequency range of 1–1000 kHz. As shown in Figure 6, the impedance of a 50-bilayer film of Ag–PAMAM/DR coated on a copper electrode was 720 ohm (conductivity was between 10^{-3} and 10^{-4} S/cm). In contrast, a PAMAM–DR multilayer film, which did not contain Ag nanoparticles, was almost an isolator.

In conclusion, ultrathin film containing Ag nanoparticles was prepared by electrostatic self-assembling. Subsequent UV irradiating stabilized the film and made it strongly resistant to polar solvents. The existence of Ag nanoparticles in the film endowed it with electric conductivity. This may be of significance, as functional films containing other metals or semiconductors can be prepared similarly and stabilized by the formation of covalent crosslink networks. Further, the stability of such functional films would make their application in different environments more practicable.

We thank Professor Gaoyuan Wei for many useful suggestions.

References

1. Jansen, J. F. G. A.; Meijer, E. W.; de Brabander-vanden Berg, E. M. M. Macromol Symp 1996, 102, 27.

2. Vooigtle, F.; Gestermann, S.; Hesse, R.; Schwierz, H.; Windisch, B. Prog Polym Sci 2000, 25, 987.
3. Garcia, M. E.; Baker, L. A.; Crooks, R. M. Anal Chem 1999, 71(1), 256.
4. Balogh, L.; Tomalia, D. A. J Am Chem Soc 1998, 120, 7355.
5. Esumi, K.; Suzuki, A.; Yamahira, A.; Torigoe, K. Langmuir 2000, 16, 2604.
6. He, J.-A.; Valluzzi, R,; Yang, K.; Dolukhanyan, T.; Sung, C.; Kummar, J.; Tripathy, S. K. Chem Mater 1999, 11, 3268.
7. (a) Wang, J. F.; Chen, J. Y.; Jia, X. R.; Cao, W. X.; Li, M. Q.; Wei, Y. Chem Commun 2000, 511. (b) Zhong, H.; Wang, J. F.; Jia, X. R.; Li, Y.; Qin, Y.; Chen, J. Y.; Zhao, X. S.; Cao, W. X.; Li, M. Q.; Wei, Y. Macromol Rapid Commun 2001 22, 583.
8. (a) Tomalia, D. A.; Baker, H.; Dewald, J. R.; Hall, M.; Kallos, G.; Martin, S.; Roeck, J.; Ryder, J.; Smith, P. Macromolecules 1986, 19, 2466. (b) Tomalia, D. A.; Baker, H.; Dewald, J. R.; Hall, M.; Kallos, G.; Martin, S.; Roeck, J.; Ryder, J.; Smith, P. Polym J (Tokyo) 1985, 17, 117.
9. Wang, R. ; Chen, J.; Cao, W. J Appl Polym Sci 1999, 74, 189.
10. Mao, G.; Tsao, Y.; Tirrell, M.; Davis, H. T.; Hessel, V.; Ringsdorf, H. Langmuir 1993, 9, 3461.
11. Fukada, K.; Shibasaki, Y.; Nekahara, H.; Endo, H. Thin Solid Films 1989, 179, 103.
12. Sun, L.; Crooks, R. M. Langmuir 1993, 9, 1951.
13. Zhao, M. Q.; Sun, L.; Crooks, R. M. J Am Chem Soc 1998, 120, 4877.
14. Esumi, K.; Suzuki,A.; Aihara, N.; Usui, K.; Torigoe, K. Langmuir 1998, 14, 3157.
15. Doremus, R. H.; Rao, P. J Mater Res 1996, 11, 2834.